Energy Conversion Circuit Laboratory

ELSEVIER

Available online at www.sciencedirect.com

ScienceDirect

Solar Energy 122 (2015) 1235–1244

SOLAR ENERGY

www.elsevier.com/locate/solener

A novel datasheet-based parameter extraction method for a single-diode photovoltaic array model

Jun-Young Park, Sung-Jin Choi *

School of Electrical Engineering, University of Ulsan, 93 Daehak-ro, Nam-gu, Ulsan 680-749, Republic of Korea

Received 12 June 2015; received in revised form 4 October 2015; accepted 2 November 2015
Available online 19 November 2015

Communicated by: Associate Editor Frank Nuesch

Abstract

This paper presents an effective parameter extraction algorithm for photovoltaic (PV) panels based only on datasheet values, which is very useful in the development phase of a power conditioning system (PCS). In order to increase the accuracy of a PV circuit model, especially in the vicinity of the maximum power point (MPP), the objective function incorporating the MPP error is formulated in the single-diode model, and a pattern search algorithm is utilized to optimize the parameters. In addition, the parameter search region and initial value are also discussed and criteria for the model accuracy in the MPP region are established. Comparison study using measurement data from the crystalline PV panel shows that the proposed method is a more accurate, uniform, and faster method of parameter extraction that is less dependent on the panel type and user skill. Furthermore, with a simple modification, this method successfully describes the PV characteristics even for various temperatures and irradiation levels in addition to the standard test condition (STC).

Keywords: Photovoltaic panel; Single-diode model; Parameter extraction; Pattern search optimization

1. Introduction

The output characteristic of a real photovoltaic (PV) panel is highly non-linear and depends on ambient temperature and irradiation level. Therefore, instead of real panels, a PV equivalent circuit model is a very powerful tool in the development phase of a power conditioning system (PCS). Among the performance measures of a PV model, the accuracy near the maximum power point (MPP) is the most important because a PCS usually adopts MPP tracking (MPPT) to maximize the utilization of the PV panels during the daytime, which increases the overall efficiency of the photovoltaic system (Cubas et al., 2014).

Among the various methods used to determine the PV equivalent circuit, modeling techniques based on only datasheet values are practically valuable because they can be used to extract circuit parameters for a real PV panel without additional measurements, and they provide rapid performance estimation with high accuracy (Wagner, 1999; Kezzar et al., 2014; Xiao et al., 2004; Crispim et al., 2007; Villalva et al., 2009; Siddique et al., 2013; Sera et al., 2007; Chan and Phang, 1987; Park and Kim, 2014). By investigating the limitations of conventional works, this paper presents a more effective method for parameter extraction in datasheet-based modeling.

2. Problem definition

A PV panel can generally be described using a single-diode model that has a current source with a diode in

* Corresponding author. Tel.: +82 52 259 2716; fax: +82 52 259 1686.
E-mail address: sjchoi@ulsan.ac.kr (S.-J. Choi).

http://dx.doi.org/10.1016/j.solener.2015.11.001
0038-092X/

parallel, as shown in Fig. 1(a). This model accounts for the non-linear I–V characteristic of a PV panel (Ouennoughi and Chegaar, 1999; Chegaar et al., 2001). The equation to determine the I–V characteristic is

$$i = I_{ph} - I_o\left(e^{\frac{v+iR_s}{N_s A V_T}} - 1\right) - (v + iR_s)G_{sh} \quad (1)$$

where V_T is the thermal voltage of the diode. In order to represent a PV panel using the single-diode model, the five circuit parameters of photovoltaic current (I_{ph}), dark saturation current (I_o), series resistance (R_s), shunt conductance (G_{sh}), and diode ideality factor (A) must be determined only from the panel datasheet, which specifies the number of cells (N_s), the voltage at maximum power (V_{mpp}), the current at maximum power (I_{mpp}), the open circuit voltage (V_{oc}), and the short circuit current (I_{sc}). Some papers also describe the shunt conductance (G_{sh}) as the inverse of shunt resistance (R_{sh}). Using these values, a PV circuit model that provides almost the same I–V characteristic as that of the real PV panel can be obtained.

Many researchers have presented parameter extraction methods that make use of four conditions provided in datasheets:

(1) The I–V curve passes through the MPP.
(2) The slope of the P–V curve is null at the MPP.
(3) The I–V curve starts at (V_{oc}, 0).
(4) The I–V curve ends at (0, I_{sc}).

These conditions are graphically demonstrated in Fig. 1(b). The extraction of I_o and I_{ph} according to conditions (3) and (4) is straightforward. However, obtaining the other three parameters, R_s, G_{sh}, and A, is rather complicated because there are only two conditions available for determining three unknowns. Furthermore, a numerical method is necessary for solving the simultaneous equations because of their implicit form.

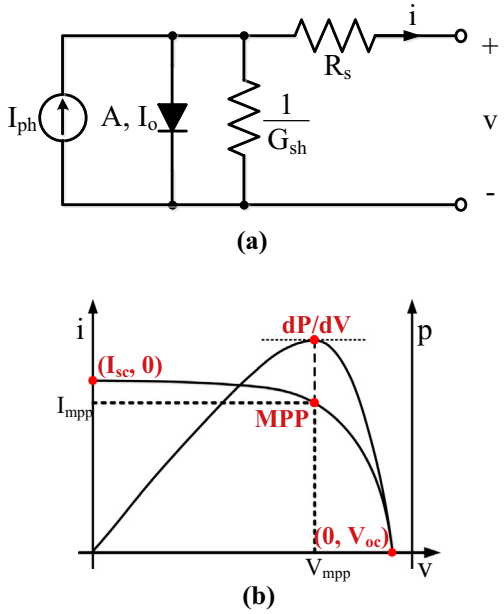

Fig. 1. Characteristic of a PV panel. (a) Single-diode model, (b) critical points in the I–V curve.

3. Conventional algorithm

Many researchers investigated effective algorithms in order to solve the under-determined situation of the PV modeling and they can be were classified under three different groups.

In the first group, they reduced the number of parameters such that the number of unknown equals to the number of constraints, and extract model parameters by solving simultaneous equations (Wagner, 1999; Kezzar et al., 2014; Xiao et al., 2004; Crispim et al., 2007). For example, Wagner (1999) assumed G_{sh} to be very low and thus excluded it from the equivalent circuit as shown in Fig. 2(a). Although such technique simplifies calculation steps and thus is computationally very fast, it inevitably shows poor accuracy for some PV panels due to the reduced number of model parameters. Therefore, it does not always guarantee the model accuracy.

Instead of omitting model parameter, the other group fixed the unknown parameter to a reasonable value in advance (Villalva et al., May 2009; Siddique et al., 2013). For example, the diode ideality factor (A) can be set before

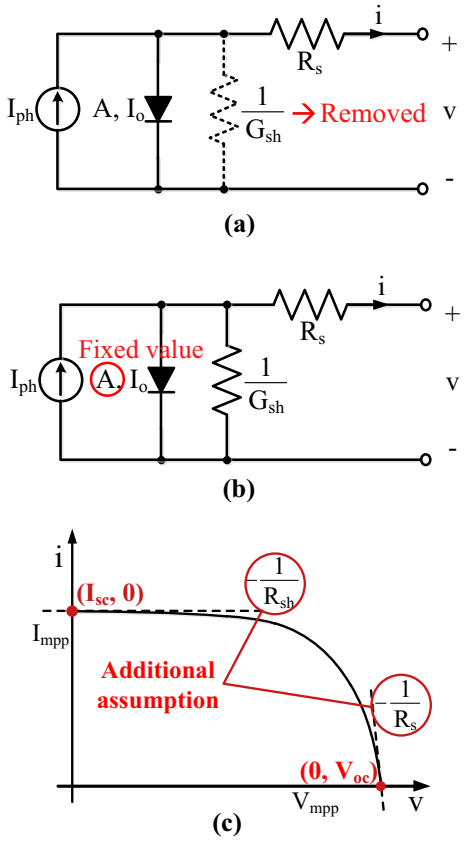

Fig. 2. Key concepts in conventional algorithms. (a) group I, (b) group II, (c) group III.

beginning the extraction process as shown in Fig. 2(b). Among them, Villalva (Villalva et al., 2009) shows good accuracy with reduced complexity. However, the choice of diode ideality factor heavily relies on user's skill and experience, so an inappropriate selection can lead to incorrect model parameters. In order to clarify this limitation, different P–V curves for a PV panel (KC200GT) are obtained by Villalva method in case of different assumption of A's and plotted in Fig. 3(a). Although the maximum value is constant, P–V curve is slightly changed according to the A value.

The third group introduced an extra slope condition of the I–V curve at the short circuit point (Sera et al., 2007; Chan and Phang, 1987) or the open circuit point (Park and Kim, 2014) as shown in Fig. 2(c), which makes the number of unknown parameters equal to the number of conditions For example, Pedro (Sera et al., 2007) used the assumption that the shunt resistance of the model can be obtained by an inverse of the tangential slope evaluated at short circuit point in an I–V curve. However, an approximation made at the far ends of the I–V curve does not guarantee model accuracy in the MPP region. Fig. 3(b) illustrates possible error caused by adopting this approximation. It shows an I–V curve for a PV panel (KC65GT) predicted by Pedro method. Consequently, conventional approaches result in performance degradation in terms of model accuracy especially near MPP. In order to enhance the accuracy, a new method is introduced in the following section.

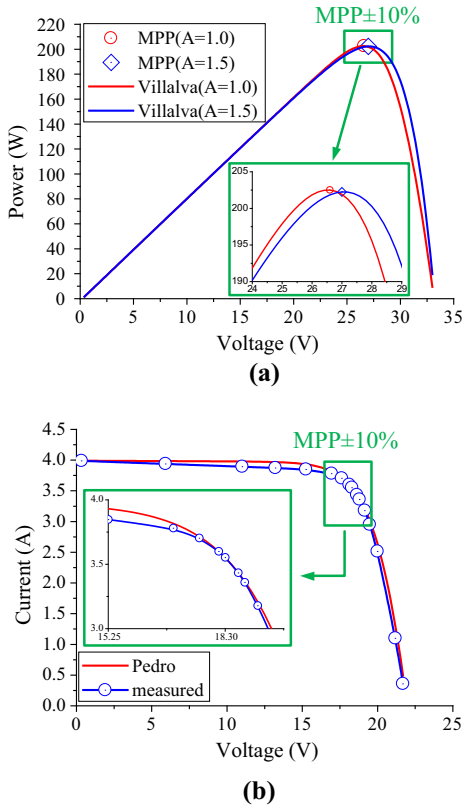

Fig. 3. Possible error caused by conventional algorithms. (a) group II, (b) group III.

4. Proposed algorithm

Fig. 4 shows the overview of the proposed algorithm. At first, datasheet values are divided into two groups: MPP-related constraints and endpoint constraints. The MPP constraints are (1) the I–V curve passes through the MPP, and (2) the slope of the P–V curve is null at the MPP. The endpoint constraints are (3) the I–V curve starts at (V_{oc}, 0), and (4) the I–V curve ends at (0, I_{sc}). The former poses an under-determined problem set solved by optimization techniques that extract circuit parameters without reducing the number of parameters, fixing one of the parameters, or introducing an extra approximate condition. The latter are reduced into simple simultaneous equations with trivial solutions. Consequently, 5 unknown circuit parameters are obtained from only 4 datasheet conditions.

4.1. Objective function definition

In this subsection, the objective function is derived from the MPP constraints. Applying condition (1) to Eq. (1), the following equation holds:

$$I_{mpp} = I_{ph} - I_o e^{\frac{V_{mpp}+I_{mpp}R_s}{N_s A V_T}} - (V_{mpp} + I_{mpp}R_s)G_{sh} \tag{2}$$

The above equation can be reformulated in a new implicit form:

$$f(R_s, G_{sh}, A) - I_{mpp} = 0 \tag{3}$$

On the other hand, the output power of a solar array can be described as a function of output voltage:

$$p(v) = iv. \tag{4}$$

From the above equation, the first derivative of the P–V relation results in

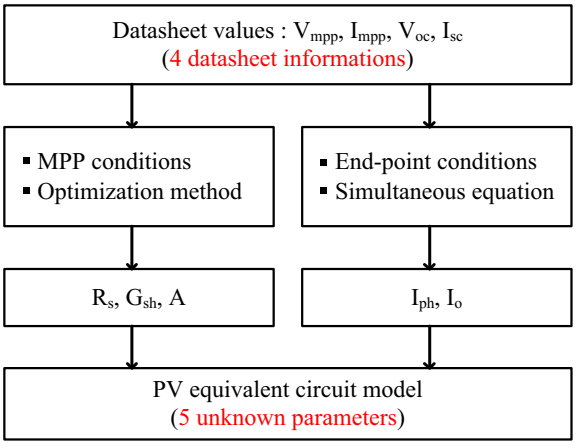

Fig. 4. Overview of the proposed algorithm.

$$\frac{dp}{dv} = \frac{d(iv)}{dv} = i + \frac{di}{dv}v. \tag{5}$$

Therefore, condition (2) can be represented as Eq. (6), and its implicit form is obtained as Eq. (7).

$$\left.\frac{dp}{dv}\right|_{@mpp} = I_{mpp} - V_{mpp}\frac{G_{sh}\left(\frac{(I_{sc}/G_{sh} - V_{oc} + I_{sc}R_s)}{N_sAV_T}e^{\frac{V_{mpp}+I_{mpp}R_s-V_{oc}}{N_sAV_T}} + 1\right)}{1 + R_sG_{sh}\left(\frac{(I_{sc}/G_{sh} - V_{oc} + I_{sc}R_s)}{N_sAV_T}e^{\frac{V_{mpp}+I_{mpp}R_s-V_{oc}}{N_sAV_T}} + 1\right)} = 0 \tag{6}$$

$$g(R_s, G_{sh}, A) = 0 \tag{7}$$

Combining Eqs. (3) and (7), an objection function is defined as Eq. (8), and the optimal values of R_s, G_{sh}, and A that minimize this function are determined so that those three parameters simultaneously best match conditions (1) and (2). In other words, determining the R_s, G_{sh}, and A using only the MPP constraints is now possible.

$$E(R_s, G_{sh}, A) \equiv \left(f(R_s, G_{sh}, A) - I_{mpp}\right)^2 + g^2(R_s, G_{sh}, A) \tag{8}$$

Meanwhile, the remaining two parameters, I_o and I_{ph}, can be directly obtained from the endpoint constraints. From Eq. (1) and conditions (3) and (4), the following two equations are obtained:

$$I_{sc} = I_{ph} - I_o e^{\frac{I_{sc}R_s}{N_sAV_T}} - I_{sc}R_sG_{sh} \tag{9}$$

$$I_{ph} = I_o e^{\frac{V_{oc}}{N_sAV_T}} + V_{oc}G_{sh}. \tag{10}$$

By eliminating I_{ph} in Eqs. (9) and (10) with the assumption that $V_{oc} >> I_{sc}R_s$, which is widely accepted in many papers, I_o can be obtained as

$$I_o = [I_{sc} - (V_{oc} - I_{sc}R_s)G_{sh}]e^{-\frac{V_{oc}}{N_sAV_T}}. \tag{11}$$

4.2. Parameter search region and initial value

Any numerical method to solve non-linear problems needs to specify a search region for the parameter variables. To implement the proposed algorithm, the search regions for R_s, G_{sh}, and A should be properly defined. The search range should not only be easily determined from the datasheet, but also physically meaningful. First, the series resistance, R_s, is ideally zero when there is no series loss. Its maximum value can be graphically obtained using the slope of a straight line connecting the short circuit point and MPP. Accordingly, the search range for R_s is given as

$$0 \leqslant R_s \leqslant \frac{V_{oc} - V_{mpp}}{I_{mpp}}. \tag{12}$$

Likewise, the shunt conductance, G_{sh}, has zero value when there is no leakage loss in the PV panel, and its maximum possible value can found in a similar fashion. Therefore, the search range for G_{sh} will be given as

$$0 \leqslant G_{sh} \leqslant \frac{I_{sc} - I_{mpp}}{V_{mpp}}. \tag{13}$$

The diode ideality factor, A, is inherent from the material characteristic. For a silicon PV panel, it is better to define the search range for A as:

$$0 < A \leqslant 2. \tag{14}$$

The objective function defined in Eq. (8) is highly non-linear and can cause a convergence issue in optimization algorithms, so the initial value of the solution should be carefully selected in order to prevent such issues. In this algorithm, it is reasonable to choose an initial search vector having ideal values for each parameter as follows:

$$X_1 = [R_{s,1}G_{sh,1}A_1] = [0, 0, 1]. \tag{15}$$

4.3. Pattern search optimization algorithm

Among the various methods (Peng et al., 2014; Ismail et al., 2013; Ishaque and Salam, 2011; Yuan et al., 2014; Soon and Low, 2012) to minimize the 3-dimensional objective function given by Eq. (8), pattern search optimization was chosen. Because this method does not employ differentiation process of the objective function and any multi-dimensional problem is solved by sequences of 1-dimensional sub-problems, it is quite robust and simple, and thus can be easily implemented. Additionally, it shows good performance in short computation time (Venkataraman, 2009).

In the pattern search algorithm, the solution vector, X_i, successively reaches the next solution $X_{i+1} = X_i + \alpha_i S_i$ using the search vector, S_i, in the direction of the unit vector of each parameter variable, i.e., $S_1 = [1,0,0]$ for R_s, $S_2 = [0,1,0]$ for G_{sh}, and $S_3 = [0,0,1]$ for A. The search direction is cycled through the number of variables in an orderly manner, executing one additional search direction as the sum of the scalar product of the previous search directions. During this process, the scalar multiplier, α_i, is determined in order to minimize the 1-dimensional objective function, $E(X_{i+1})$. In this step to solve the single-variable minimization problem, α_i is determined using the golden section algorithm.

A flow chart of the proposed parameter extraction algorithm incorporating pattern search optimization is summarized in Fig. 5. If the termination conditions of the algorithm

$$|\Delta E| \leqslant \varepsilon_1 \tag{16}$$

$$\Delta X^T \Delta X \leqslant \varepsilon_2 \tag{17}$$

are met with $\varepsilon_1 = \varepsilon_2 = 1 \times 10^{-8}$, the algorithm concludes with the optimal parameters. The termination conditions are based on the function decrease in each cycle and the change in the parameter variable.

5. Performance result

To evaluate the performance of the proposed algorithm, nine crystalline PV samples – THERM Solartechnik AT50, BP Solar MSX60, Kyocera KC65GT, BP Solar MSX120,

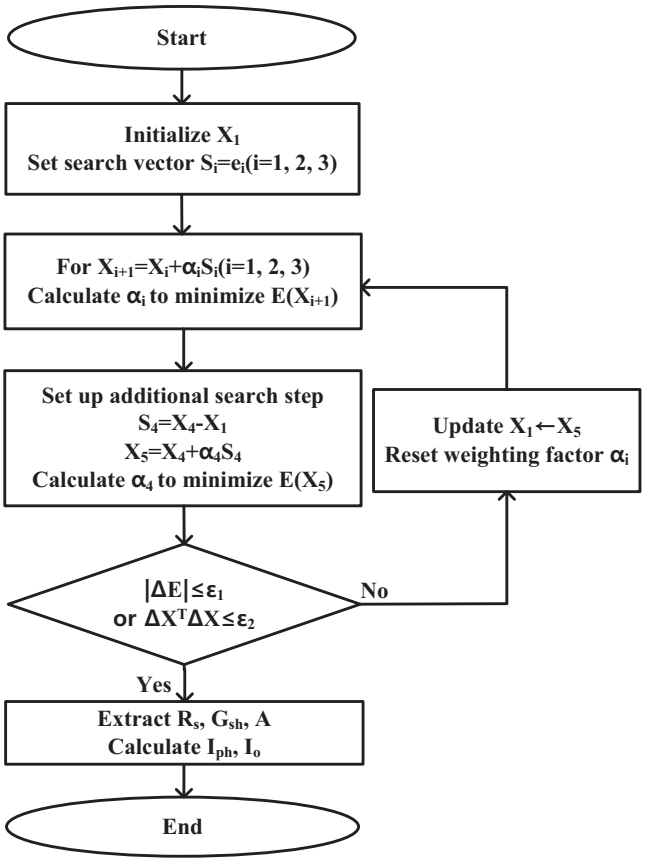

Fig. 5. Flow chart of the proposed algorithm.

Shell Solar SQ160PC, Kyocera KC200GT, Samsung LPC241SM, Trina Solar TSM245PC, and Hanwha Solar SF260 – are selected to extract PV circuit models. The datasheet values of each panel are shown in Table 1. Using only the datasheet values, the three conventional methods in Wagner, Villalva, and Pedro and the proposed method are tested using the following steps.

First, from the I_{sc}, V_{oc}, I_{mpp}, V_{mpp}, and N_s values provided in datasheets, the parameters of the PV model for each panel are extracted using individual algorithms implemented with MATLAB m-script. Secondly, those extracted values are used to obtain the simulated I–V and P–V curves through the PSIM circuit blocks from Villalva et al. (2009), PSIM User's Guide (2010), as shown in Fig. 6. Finally, the characteristic curves of the PV model are plotted in Figs. 7 and 8 together with the measured data from a real PV panel. Because the model accuracy of Villalva method heavily depends on the selection of the diode ideality factor, different values for A are used, and the one that shows the best performance is chosen in each plot.

To obtain measured data, most of literature (Wagner, 1999; Kezzar et al., 2014; Xiao et al., 2004; Crispim et al., 2007; Villalva et al., 2009; Siddique et al., 2013; Sera et al., 2007; Chan and Phang, 1987; Park and Kim, 2014) which studies datasheet-based parameter extraction usually utilizes the only datasheet values. This is because datasheet values are already measured in compliant to standard test condition (STC) – cell temperature of 25 °C, sunlight of 1000 W/m^2, and air mass of 1.5 – which is suggested by EN standard and repeating the experiments just for extracting the PV characteristic is redundant work and also prone to additional error. In this paper, all measurement data are directly obtained from the curve shown in PV panel datasheets except for AT50 panel whose data are reconstructed from literature (Park and Kim, 2014).

Figs. 7 and 8 show that, even if each algorithm shows slightly different trends in the I–V and P–V curves, it is difficult to determine the best algorithm without using predetermined criteria. Therefore, it is necessary to establish a measure of model accuracy, especially for the region in the vicinity of the MPP, and EN50530 can be used as the basis (IEC EN50530). This standard states that the actual I–V characteristic of the PV simulator must not deviate by more than 1% from the rated output power within the voltage range from $0.9V_{mpp}$ to $1.1V_{mpp}$ ($V_{mpp} \pm 10\%$) related to the predetermined characteristic. To assess the accuracy of each algorithm according to this standard, the current error and power error in the MPP region are introduced in Eqs. (18) and (19):

$$\varepsilon_I(\%) = \frac{1}{0.2V_{mpp}} \int_{V_{mpp}\pm 10\%} \left| \frac{i_s(v) - i_m(v)}{i_m(v)} \right| dv \cdot 100 \tag{18}$$

$$\varepsilon_P(\%) = \frac{1}{0.2V_{mpp}} \int_{V_{mpp}\pm 10\%} \left| \frac{p_s(v) - p_m(v)}{p_m(v)} \right| dv \cdot 100. \tag{19}$$

where the subscripts 'm' and 's' denote the measured and simulated values, respectively. To implement the numerical

Table 1
Datasheet values of PV panels.

	I_{sc} (A)	V_{oc} (V)	I_{mpp} (A)	V_{mpp} (V)	P_{mpp} (W)	N_s	k_i (A/°C)	k_v (mV/°C)
AT50	3.3	21.5	2.86	17.5	50	39	–	–
MSX60	3.8	21.1	3.5	17.1	60	36	$2.47 \cdot 10^{-3}$	−80
KC65GT	3.99	21.7	3.75	17.4	65	36	$1.59 \cdot 10^{-3}$	−82.1
MSX120	3.87	42.1	3.52	33.7	120	72	$2.47 \cdot 10^{-3}$	−80
SQ160PC	4.9	43.5	4.58	35	160	72	$1.4 \cdot 10^{-3}$	−161
KC200GT	8.21	32.9	7.66	26.7	200	54	$3.18 \cdot 10^{-3}$	−123
LPC241	8.54	37.4	8.01	30.1	241	60	$2.135 \cdot 10^{-3}$	−127.5
TSM245	8.68	37.5	8.13	30.2	245	60	$4.0796 \cdot 10^{-3}$	−120
SF260	8.4	44.3	7.76	36.1	280	72	$3.104 \cdot 10^{-3}$	−115.52

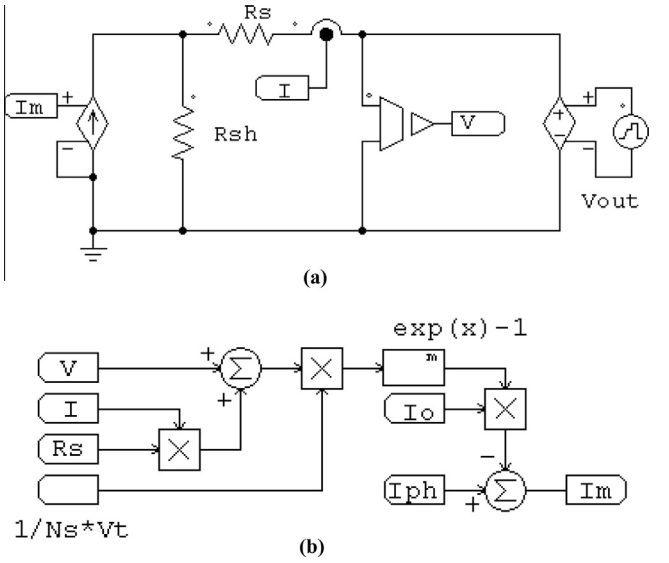

Fig. 6. PSIM implementation to simulate the characteristic curve. (a) equivalent circuit, (b) parameter calculation.

integration in Eqs. (18) and (19), the trapezoidal rule is used.

Performance comparisons regarding model accuracy are shown in Fig. 9(a) and (b). While Wagner method shows large error in AT50, KC65GT, KC200GT, and TSM245PC, Pedro method has large error in AT50, MSX120, KC65GT, and TSM245PC and needs long calculation time. Villalva method shows improved results in both accuracy and calculation time, but it still shows large current error in KC65GT and KC200GT and incorrect results especially in power error. Therefore, it is clear from the results that even if one algorithm shows good accuracy for certain PV samples, it may show poor accuracy for other samples.

Because users usually have no idea of which algorithm should be adopted in advance, crucial and demanding feature for the algorithm is the uniform model accuracy. The proposed algorithm shows high accuracy, and what's more, its performance is relatively independent of individual solar-panels. To prove the superiority, we introduced statistical indices such as average error (E), standard deviation of error (σ). Because larger standard deviation not always means poor uniformity, the third index called "coefficient of variation", defined by the ratio of the standard deviation to average value, is introduced to measure the uniformity of the results. The results are summarized in Table 2. The average data shows that the proposed method shows better accuracy than other methods. Moreover, its lower coefficient of variance shows that it provides more uniform model accuracy. As predicted in Section 3, conventional methods show relatively poor performance due to the way how they solved the underdetermined parameter extraction problem.

Fig. 9(c) compares the parameter extraction time for simulations performed using an Intel i5 760 2.80 GHz processor, where Wagner method is excluded in the plot

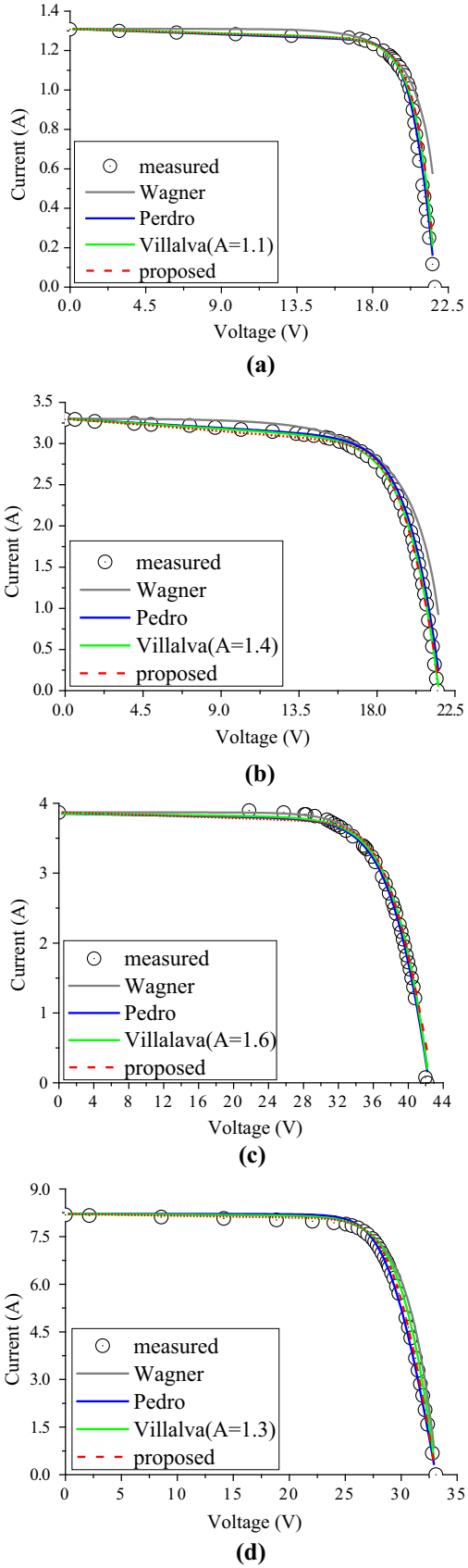

Fig. 7. I–V characteristic curve. (a) SLP020, (b) AT50, (c) MSX120, (d) KC200GT.

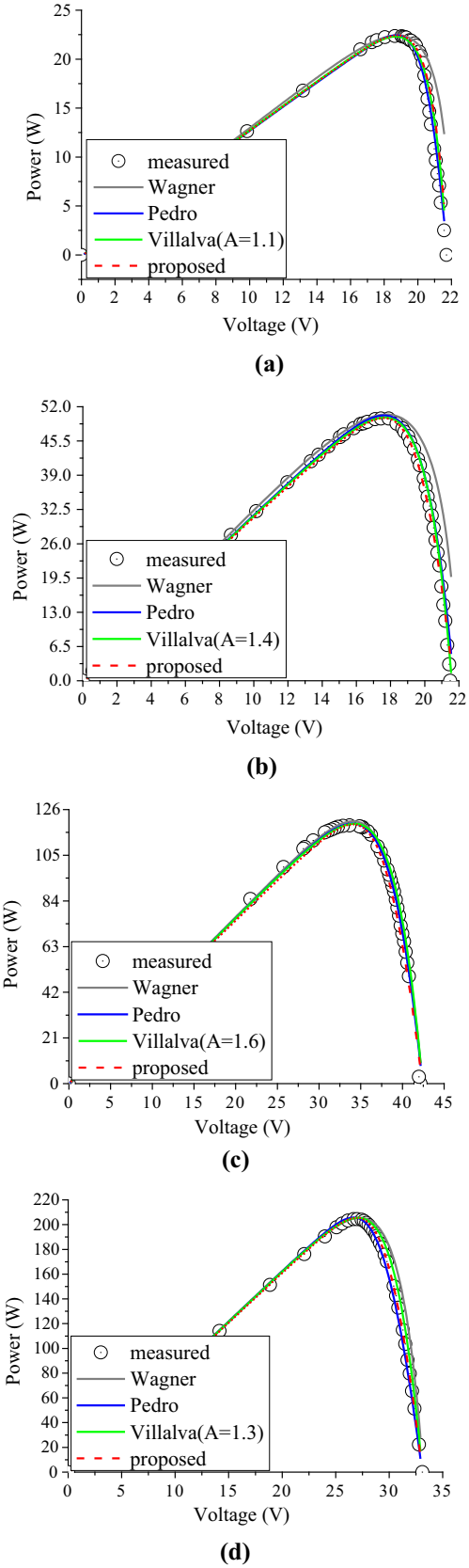

Fig. 8. *P–V* characteristic curve. (a) SLP020 (b) AT50, (c) MSX120 (d) KC200GT.

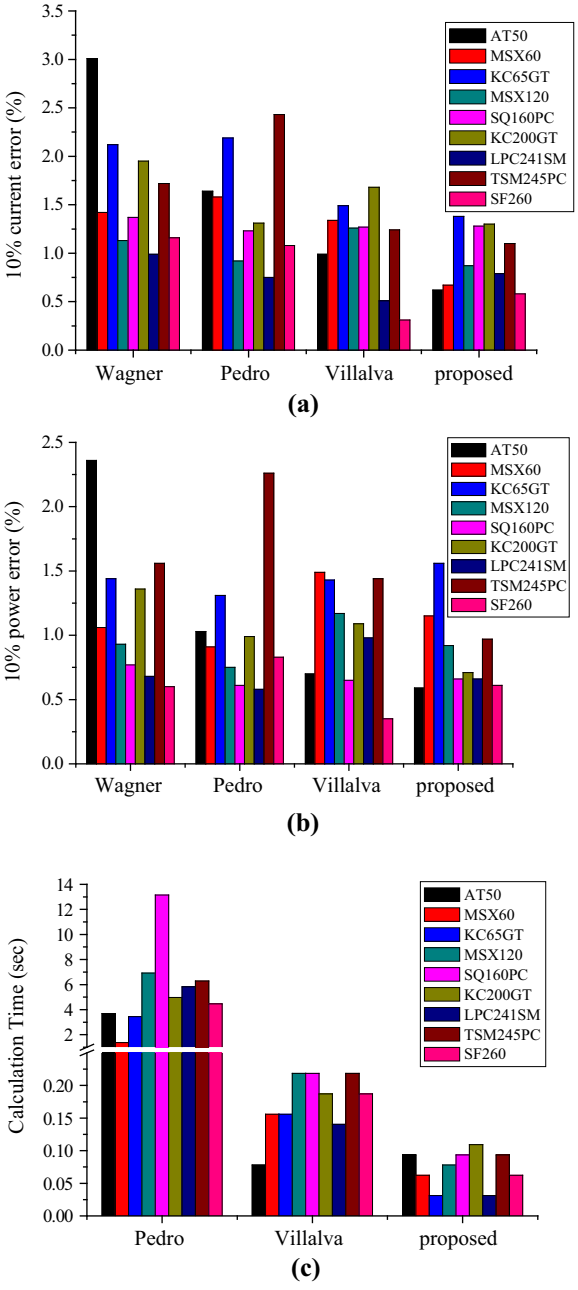

Fig. 9. Comparisons of algorithm performance. (a) 10% current error, (b) 10% power error, (c) extraction time.

because it is a non-iterative algorithm. The proposed algorithm shows the best performance among all of them. Variations in the extracted parameters for KC200GT and the corresponding value of the objective function with respect to the iteration steps of the proposed method are shown in Fig. 10. Through the iteration process, the unknown parameter converges, and the parameters for the PV single-diode model are extracted within 41 steps. Consequently, the proposed algorithm provides an accurate, uniform, and rapid parameter extraction solution for the single-diode model of PV panels.

Table 2
Statistical verification for each algorithm.

	Current error (%)			Power error (%)			Calculation time (s)		
	E	σ	σ/E	E	σ	σ/E	E	σ	σ/E
Wagner	1.652	0.637	0.385	1.196	0.555	0.464	–	–	–
Pedro	1.459	0.563	0.386	1.03	0.513	0.498	3.3	5.571	0.592
Villalva	1.121	0.447	0.399	1.033	0.4	0.387	0.046	0.173	0.268
Proposed	0.954	0.315	0.33	0.87	0.321	0.37	0.028	0.073	0.386

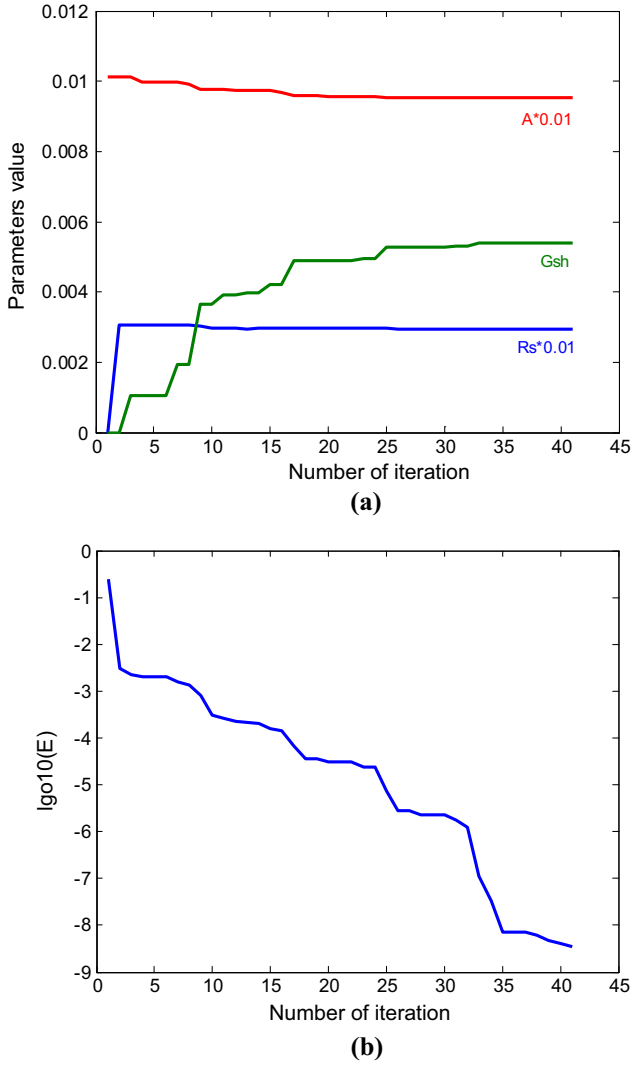

Fig. 10. Optimization process of the proposed method in KC200GT. (a) Parameter convergence, (b) objective function evaluation.

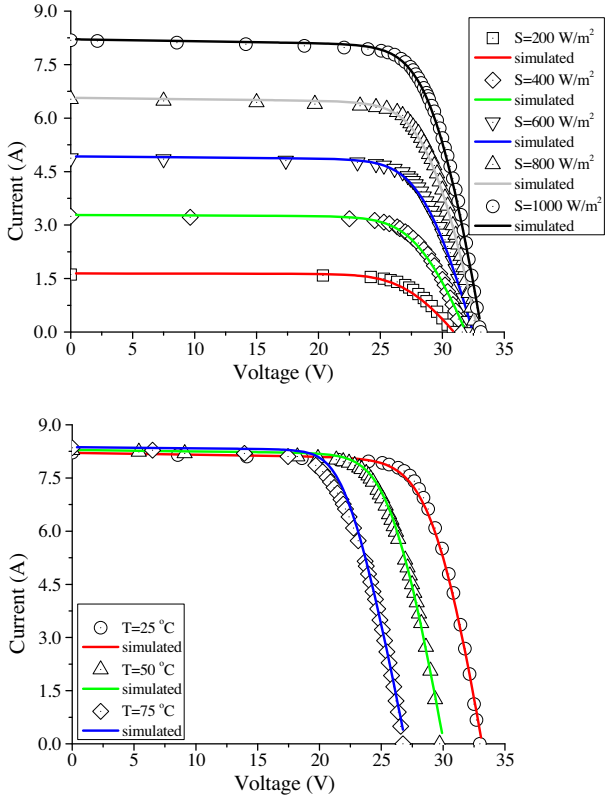

Fig. 11. I–V and P–V characteristic curves of KC200GT panel at varying irradiation values.

6. Temperature and irradiation dependence

Usually, datasheet values are measured in STC – cell temperature of 25 °C, sunlight of 1000 W/m^2, and air mass of 1.5 – and the characteristics of a PV panel deviate according to the ambient temperature and irradiation level. For the temperature compensation, datasheet specifies temperature coefficients only for the endpoints of the PV curve such as k_i for I_{sc} and k_v for V_{oc}. The manufacturer usually does not provide the temperature dependencies of MPP, but the following approximations have been reported to be valid (Soon and Low, 2012; King et al., 1997).

$$k_{i,mpp} \cong k_i, k_{v,mpp} \cong k_v \tag{20}$$

where $k_{i,mpp}$ and $k_{v,mpp}$ are the temperature coefficients of I_{mpp} and V_{mpp}, respectively.

For the compensation of irradiation level, it is also known that I_{sc} from the PV panel is directly proportional to the irradiation level as

$$I_{sc} = I_{sc,STC}\frac{S}{S_{STC}} \tag{21}$$

where S is the irradiation level and the subscript 'STC' stands for its value in STC. The dependency of V_{oc} on the irradiation condition is known to have a logarithmic proportionality (De Soto et al., 2007; Celik and Acikgoz, 2007; Gonzalez-Moran et al., 2009) and is approximated as

$$V_{oc} = V_{oc,STC} + N_s A_{STC} V_T ln\left(\frac{S}{S_{STC}}\right) \quad (22)$$

where A_{STC} is the diode ideality factor that has been extracted from the datasheet.

Therefore, datasheet values should be updated to include the temperature and irradiation effects in the following manner:

$$I_{sc} = I_{sc,STC}\frac{S}{S_{STC}}[1 + k_i(T - T_{STC})] \quad (23)$$

$$V_{oc} = V_{oc,STC} + N_s A_{STC} V_T ln\left(\frac{S}{S_{STC}}\right) + k_v(T - T_{STC}) \quad (24)$$

$$I_{mpp} = I_{mpp,STC}\frac{S}{S_{STC}}[1 + k_{i,mpp}(T - T_{STC})] \quad (25)$$

$$V_{mpp} = V_{mpp,STC} + N_s A_{STC} V_T ln\left(\frac{S}{S_{STC}}\right) + k_{v,mpp}(T - T_{STC}) \quad (26)$$

where T is the operating temperature and the subscript '*STC*' stands for its value in *STC*.

According to the updated equations, the proposed method extracts new parameter values depending on temperature and irradiation conditions. To verify this approach, the PV characteristic curves in various environmental conditions are simulated and compared with measure data in Figs. 11–13 for KC65GT, KC200GT, and SQ160PC, respectively. The measured points are obtained from the manufacturer's datasheets. It is clear that the proposed algorithm successfully describes the characteristic of a real PV panel even in conditions other than the STC.

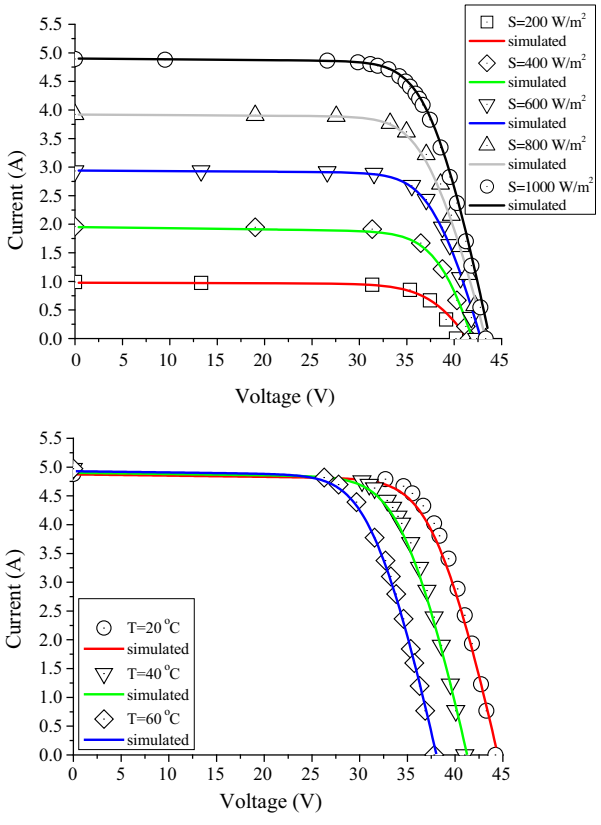

Fig. 12. *I–V* and *P–V* characteristic curves of SQ160PC panel at varying irradiation values.

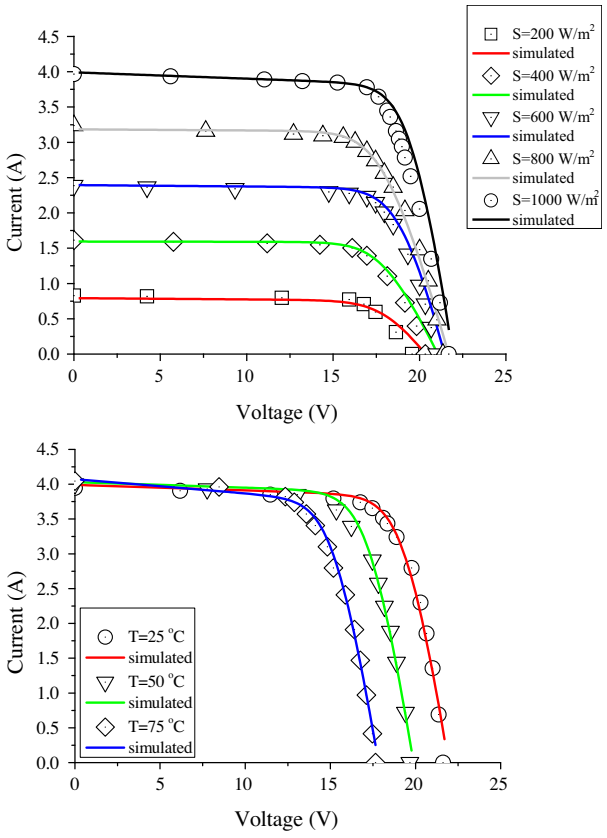

Fig. 13. *I–V* and *P–V* characteristic curves of KC65GT panel at varying irradiation values.

7. Conclusion

This paper presents an effective parameter extraction method for a single-diode PV model using only the datasheet values of real PV panels. In order to enhance the model accuracy, especially for the MPP region, the datasheet information is divided into MPP and endpoint constraints. The former are solved using pattern search optimization with an objective function specifying only the MPP conditions, and the latter are solved using multiple simultaneous equations. The performance comparison of the current error and the power error near the MPP according to EN50530 verifies that this algorithm provides good accuracy irrespective of the individual PV panel characteristics. Therefore, the presented method provides uniform method for parameter extraction that is less dependent on the panel type and skill of users. Furthermore, the implementation is simple, and the extraction time is very short. Additionally, with simple updated equations for the datasheet values, the proposed method shows great

accuracy even under temperature and irradiation conditions different from STC.

Acknowledgement

This work was supported by the 2013 Research Fund of University of Ulsan, Republic of Korea.

References

Celik, A.N., Acikgoz, N., 2007. Modeling and experimental verification of the operating current of mono-crystalline photovoltaic modules using four- and five-parameter models. Appl. Energy 84 (1), 1–5.

Chan, D., Phang, J., 1987. Analytical methods for the extraction of solar cell single- and double-diode model parameters. IEEE Trans. Electron. Dev. 34 (2), 286–293.

Chegaar, M., Ouennoughi, Z., Hoffmann, A., 2001. A new method for evaluating illuminated solar cel parameters. Solid-State Electron. 45, 293–296.

Crispim, J., Carreira, M., Castro, R., 2007. Validation of Photovoltaic Electrical Models against Manufacturer's Data and Experimental Results. In: International Conference on Power Engineering, Energy and Electrical Drives.

Cubas, J., Pindado, S., Victoria, M., 2014. On the analytical approach for modeling photovoltaic systems behavior. J. Power Sources 247, 467–474.

De Soto, W., Klein, S.A., Beckman, W.A., Jan. 2007. Improved and validation of a model for photovoltaic array performance. Sol. Energy 81 (1), 78–88.

Gonzalez-Moran, C., Arboleya, P., Reigosa, D., Diaz, G., Gomez-Alexandre, J., 2009. Improved Model of Photovoltaic Sources considering ambient Temperature and Solar Irradiation. In: IEEE PES/IAS Conference on Sustainable Alternative Energy.

IEC EN50530, Standard for Overall Efficiency of Photovoltaic Inverters, CENELEC, Stassart 35, B-1050 Brussels.

Ishaque, K., Salam, Z., 2011. An improved modeling method to determine the model parameters of photovoltaic (PV) modules using differential evolution (DE). Sol. Energy 85, 2349–2359.

Ismail, M.S., Moghavvemi, M., Mahlia, T.M.I., 2013. Characterization of PV panel and glabal optimization of its model parameters using genetic algorithm. Energy Convers. Manage. 73, 10–25.

Kezzar, R., Zereg, M., Khezzar, A., 2014. Modeling improvement of the four parameter model for photovoltaic modules. Sol. Energy 110, 452–462.

King, D.L., Kratochvil, J.A., Boyson, W.E., 1997. Temperature Coefficients for PV Modules and Arrays: Measurement Method, Difficulties, and Results. In: IEEE 26th Photovoltaic Specialists Conference.

Ouennoughi, Z., Chegaar, M., 1999. A simpler method for extracting solar cell parameters using the conductance method. Solid-State Electron. 43, 1985–1988.

Park, H.A., Kim, H.S., 2014. Mathematical consideration on PV cell modeling. Trans. Korean Inst. Power Electron. 19 (1).

Peng, L., Sun, Y., Meng, Z., 2014. An improved model and parameters extraction for photovoltaic cells using only three state points at standard test condition. J. Power Sources 248, 621–631.

PSIM User's Guide, Ver. 9, May 2010, POWERSIM.

Sera, D., Teodorescu, R., Rodriguez, P., 2007. PV Panel Model Based on Datasheet Values. In: IEEE International Symposium on Industrial Electronics, pp. 2392–2396.

Siddique, H.A.B., Xu, P., De Doncker, R.W., 2013. Parameter Extraction Algorithm for One-Diode Model of PV Panels based on Datasheet Values. In: International Conference on Clean Electrical Power (ICCEP).

Soon, J.J., Low, K.S., 2012. Photovoltaic model identification using particle swarm optimization with inverse barrier constraint. IEEE Trans Power Electron 27 (9).

Venkataraman, P., 2009. Applied Optimization with MATLAB Programming, second ed. WILEY.

Villalva, M.G., Gazoli, J.R., Filho, E.R., 2009. Modeling and circuit-based simulation of photovoltaic arrays. IEEE Trans. Power Electron., 1244–1254

Villalva, M.G., Gazoli, J.R., Filho, E.R., May 2009. Comprehensive approach to modeling and simulation of photovoltaic arrays. IEEE Trans. Power Electron. 24 (5), 1198–1208.

Wagner, A., 1999. Photovoltaik Engineering, Die Methode der Effektiven Solarzellen-Kennlinie. Springer-Verlag, Berlin, Heidelberg, New York.

Xiao, W., Dunford, W.G., Capel, A., 2004. A Novel modeling method for photovoltaic cells. In: IEEE 35th Annual Power Electronics Specialists Conference (PESC), vol. 3, pp. 1950–1956.

Yuan, X., Xiang, Y., He, Y., 2014. Parameter extraction of solar cell models using mutative-scale parallel chaos optimization algorithm. Sol. Energy 108, 238–251.